

Origin and frequency dependence of nonlinear optical susceptibilities of glasses*

Robert Hellwarth, Joel Cherlow, and Tien-Tsai Yang

Electronics Sciences Laboratory, University of Southern California, Los Angeles, California 90007

(Received 3 June 1974)

We have determined the frequency dependence of the nonlinear optical susceptibilities of fused quartz and four other glasses, and determined the relative contributions of "electronic" and "nuclear" mechanisms to their nonlinear optical indices. This is the first such determination in solids. Our method has been to analyze our own absolute measurement of ordinary differential Raman-scattering cross sections in conjunction with the coefficients for intensity-induced polarization changes measured by Owyong in the same glasses.

The nonlinear optical polarization density $\vec{P}^{(3)}(\vec{r}t)$, which is third order in the electric field in a material, manifests itself in a variety of commonly observed nonlinear optical effects such as beam self-focusing, self-phase modulation, frequency mixing, and intensity-induced polarization changes (IIPC). Here we point out a relation between differential Raman-scattering cross sections and $\vec{P}^{(3)}$ which we use to determine both the frequency dependence and physical origins of the nonlinear polarization in five optical glasses. This is the first such determination in solids. We use our own Raman-scattering measurements in conjunction with the IIPC data of Owyong¹ to characterize $\vec{P}^{(3)}$ for any effect at "optical" frequencies—that is, at frequencies too low to excite electronic transitions and too high for nuclear motions to follow.

Several connections between ordinary Raman scattering and specific third-order nonlinear effects have been developed and used previously. (By "Raman scattering" we mean inelastic light scattering from all nuclear motions, vibrations, rotations, librations, etc., except macroscopic density fluctuations.) For example, the induced optical parametric amplification and loss in a material from the third-order process called "stimulated Raman scattering" is known to be related to ordinary Raman scattering in the material, analogously as the resistance of a circuit element is related to its thermally induced voltage fluctuations by Nyquist's theorem.² Levenson, Flytzanis, and Bloembergen have predicted and observed the interference in three-wave mixing between the waves generated by the nonlinear "Raman" polarization of a simple-harmonic lattice vibration and by the nonlinear distortion of the electronic orbits.³ Levenson has used the interference between waves mixed by a calibrated Raman vibration in one substance with waves mixed by unknown nonlinearities of a second substance to measure the latter at a particular frequency combination.⁴ Here we use measurements of the absolute Raman-scattering

cross sections of isotropic materials (glasses) in conjunction with IIPC measurements in the same glasses to characterize $\vec{P}^{(3)}$. Our results enable us to predict any nondamaging, nonlinear optical effect involving any number of optical waves of any combination of frequencies (e.g., n -wave mixing, self-phase modulation, self-focusing, etc.) except effects arising from macroscopic density changes caused by electrostriction and heating. Furthermore, our analysis does not assume the nuclear motions are harmonic. The analysis does assume, however, that the Born-Oppenheimer (BO) approximation is valid for the states of the material. That is, we use the widely applicable assumption that, for the "optical" frequencies of interest, the electrons adiabatically follow both the nuclear motions and the changing optical fields.

In this case, there are two distinct physical contributions to $\vec{P}^{(3)}(\vec{r}t)$ (apart from electrostriction-induced strains, which we ignore). First, there is an "electronic" contribution from the nonlinear distortion of the electron orbits around the average positions of the nuclei. This polarization responds rapidly to field changes, within a few electronic cycles ($\sim 10^{-16}$ sec). In isotropic materials it contributes a term to $\vec{P}^{(3)}$ well approximated by the instantaneous form

$$\frac{1}{2}\sigma\vec{E}(\vec{r}t)E^2(\vec{r}t) \quad (1)$$

for frequencies well below the electronic band gap. The scalar coefficient σ is independent of temperature at fixed density.

A second, "nuclear," contribution arises from an optical-field-induced change in the motions of the nuclei; about these changed motions the electronic currents respond linearly to the optical fields. After the sudden impression of a field this contribution can be observed only following a time lapse of the order of the time ($\sim 10^{-12}$ sec) required for a nucleus to execute a vibrational or rotational cycle. In isotropic materials this contribution to $\vec{P}^{(3)}$ must be of the form (at some position \vec{r})⁵

$$\vec{E}(t) \int_{-\infty}^{\infty} ds a(t-s) E^2(s) + \int_{-\infty}^{\infty} ds \vec{E}(s) b(t-s) \vec{E}(t) \cdot \vec{E}(s) \quad (2)$$

for frequencies well below the electronic band gap. The nuclear response kernels, $a(t)$ and $b(t)$, vanish for $t < 0$ by causality, and generally exhibit a marked temperature dependence at constant density. The form (2) follows from the BO approximation by calculating the average over all states of the nuclei (in the ground electronic state) of the optical polarization density $\vec{\chi}(\{R_n\}) \cdot \vec{E}(t)$, expanded to first order in the BO interaction Hamiltonian $-\frac{1}{2} \vec{E}(s) \cdot \vec{\chi} \cdot \vec{E}(s)$. Here, $\vec{\chi}(\{R_n\})$ is the local optical susceptibility operator for any configuration $\{R_n\}$ of the nuclei in some microscopic region (much smaller than optical wavelengths) around \vec{r} . The superposition of (1) and (2) is a much simpler form for $\vec{P}^{(3)}$ than is required generally outside the optical Born-Oppenheimer (BO) regime considered here. We now proceed to use this simplification to relate the IIPC coefficient and Raman spectrum to the parameters σ , $a(t)$, and $b(t)$.

That $\vec{P}^{(3)}$ should cause the elliptical state of polarization of a strong monochromatic beam to change was first predicted and observed by Maker *et al.*⁶ For a plane wave of frequency ω propagating in an isotropic medium, this "intensity-induced polarization change" (IIPC) manifests itself by a rotation of the axes of the polarization ellipse through an angle $\theta(z)$ which increases with the distance z along the beam. An expression for θ in terms of σ , $a(t)$, and $b(t)$ is easily found by inserting such a plane wave E in (1) and (2), and then verifying that Maxwell's equations are satisfied (to order E^3) with this nonlinear polarization density, provided that^{1,5}

$$\theta = \frac{\pi \omega z \langle E^2(t) \rangle (\sigma + 2B_0) \cos 2\phi}{8nc}, \quad (3)$$

where c is the velocity of light, $\tan \phi$ is the ratio of right to left circular polarization amplitudes, and B_0 is the value of the Fourier transform B_Δ of $b(t)$ evaluated at $\Delta = 0$ (esu used throughout). We define $B_\Delta \equiv \int dt b(t) e^{i\Delta t}$, and A_Δ similarly. We next see how A_Δ and B_Δ can be determined from differential Raman-scattering cross sections. Knowing B_Δ and A_Δ we can determine σ , and thereby the entire nonlinear polarization (1) and (2), through IIPC measurements which according to (3) give $\sigma + 2B_0$.

Consider first the well-known nonlinear optical effect of ordinary (non-phased-matched) stimulated Raman scattering in which the presence of a strong plane polarized "pump" wave $\hat{x}F \cos(\nu t - k_0 z)$ in a medium causes a second weak wave $\text{Re} \hat{e} E \times \exp[i(\omega t - \vec{k} \cdot \vec{r})]$ to experience exponential gain. If \vec{E} in (1) and (2) is the sum of these two optical

fields, then Maxwell's equations are satisfied to order $F^2 E$ for real ν , k_0 , and ω , if \vec{k} is a complex vector $\hat{s}(k' + \frac{1}{2}i g)$ where g , the "stimulated power gain per cm," is

$$g_{\parallel} = \frac{2\pi\omega F^2}{nc} \text{Im}(A_{\Delta} + B_{\Delta}), \quad \Delta \equiv \nu - \omega \quad (4)$$

when $\hat{e} \parallel \hat{x}$, or

$$g_{\perp} = \frac{\pi\omega F^2}{nc} \text{Im} B_{\Delta}, \quad \Delta \equiv \nu - \omega \quad (5)$$

when $\hat{e} \perp \hat{x}$.

There exists a well-known relation between these stimulated gain coefficients and the differential Raman-scattering cross sections $d^2\sigma_i(\nu, \Delta)/d\Omega d\Delta$, defined as the fraction of incident photons of frequency ν inelastically scattered per unit distance into solid angle $d\Omega$ and angular frequency range $d\Delta$ about $\nu - \Delta$ when the incident and scattered polarizations are either parallel ($i = \parallel$) or perpendicular ($i = \perp$).² Substituting (4) and (5) into Eq. (4) of Ref. 2 gives the general relations which we seek:

$$\text{Im} B_{\Delta} = \frac{\pi c^4}{\hbar \nu \omega^3} \frac{d^2\sigma_{\perp}}{d\Omega d\Delta} (1 - e^{-h\Delta/kT}), \quad (6)$$

and a similar relation with A_{Δ} and $\frac{1}{2}\sigma_{\parallel} - \sigma_{\perp}$ substituted for B_{Δ} and σ_{\perp} , respectively. Because of the causal nature of $a(t)$ and $b(t)$, the real parts of their Fourier transforms can be calculated from their imaginary parts by the usual Kramers-Kronig integrals:

$$\text{Re} B_{\Delta} = \frac{1}{\pi} \int_{-\infty}^{\infty} \frac{d\nu}{\nu - \Delta} \text{Im} B_{\nu}, \quad (7)$$

and similarly for A_{Δ} .

We can see therefore from (6) and (7) how the entire transforms of $a(t)$ and $b(t)$ can be deduced from our measured Raman-scattering cross sections in Fig. 1 for the five glasses: (i) Homosil fused quartz (Amersil, Inc.), (ii) LSO (American Optical Co.), (iii) ED-4 (Owens Illinois, Inc.), (iv) SF-7 (Schott), and (v) LaSF-7 (Schott). The curves in Fig. 1 were obtained from 90° Raman-scattering measurements using the 514-nm line of an argon-ion laser and a double monochromator whose spectral sensitivity was calibrated with a quartz-iodine standard lamp. The absolute cross sections were obtained by comparison with the 992-cm⁻¹ line of liquid benzene for which the absolute cross section has been determined to within 3% by Kato and Takuma.⁷ Index corrections of the type described by these authors were performed. Our measurements of the polarized Raman cross sections of fused quartz yield Raman gains in (4) about 20% greater than those reported by Stolen and Ippen,⁸ but within their limits of error.

To obtain the values of B_0 (required to deter-

mine the electronic coefficient from IIPC measurements) and A_0 (used later to calculate the self-focusing index n_2) we use (6) in (7) finding

$$B_0 = \frac{2c^4}{\hbar\nu} \int_0^\infty \frac{d\Delta}{\omega^3 \Delta} \frac{d^2\sigma_\perp(\nu, \Delta)}{d\Omega d\Delta} (1 - e^{-\hbar\Delta/kT}) \quad (8)$$

and similarly for A_0 . Using the cross sections of Fig. 1 in (8) gives the values for A_0 and B_0 listed in Table I. Also listed there are Owyong's IIPC measurements of $\sigma + 2B_0$ (taken at 694 nm) from which we deduce the listed values of σ . The estimated absolute uncertainty of the curves of Fig. 1 is about $\pm 10\%$ for the polarized spectra and slightly greater for the depolarized spectra.

The largest contribution to this uncertainty is the uncertainty in the various absolute calibrations; the random error in the reproducibility of the shapes of the glass spectra was negligible. For this reason, the errors are probably not smoothed out by the integrating procedure and carry over to the values of B_0 and $A_0 + B_0$. In the numerical evaluations of the integral (8) we have integrated to high enough values of Δ so that the remaining tail contributed less than 1% to the integral. At the low-frequency end of the spectrum we have made the assumption that the Raman-scattering intensity decreases linearly to zero with decreasing frequency for scattered frequencies below 20 cm^{-1} . This assumption is not critical. As a check we truncated the integration at 20 cm^{-1} and found that the results differed from the others by less than 1%. Our measurements do not rule out the possibility of resonances at very low frequencies; however, we do not anticipate any large contribution from them.

It is possible that our values for A_Δ and B_Δ are up to 10% to 20% larger than their values in the long-wavelength (BO) limit. We attempted to check this by repeating our Raman measurements with the 647-nm line of the krypton laser. However, fluorescence rendered these measurements inaccurate, except in fused quartz. In this case we observed the same scattering intensity relative to benzene as we did with 514-nm excitation though experimental conditions were less reliable than in the green. Perhaps the most significant indication of the dispersion of A_Δ and B_Δ in benzene is the measured dispersion in its Kerr constant B . In the BO regime, B is proportional to $n(\sigma + B_0)/\lambda$,⁵ and for benzene $\sigma \approx 0.1B_0$.⁴ Using McComb's¹¹ eleven measurements of $B(\lambda)$ of benzene, we find that B_0 increases by $4\% \pm 3\%$ from 647 to 514 nm. McComb's dispersion data agrees with the increase of 1% in $\lambda^4 d_\sigma/d\Omega$ which Kato and Takuma observed in changing from 514 to 488 nm excitation.⁷ McComb's data do not agree, however, with the $29 \pm 6\%$ decrease in this quantity which they observed

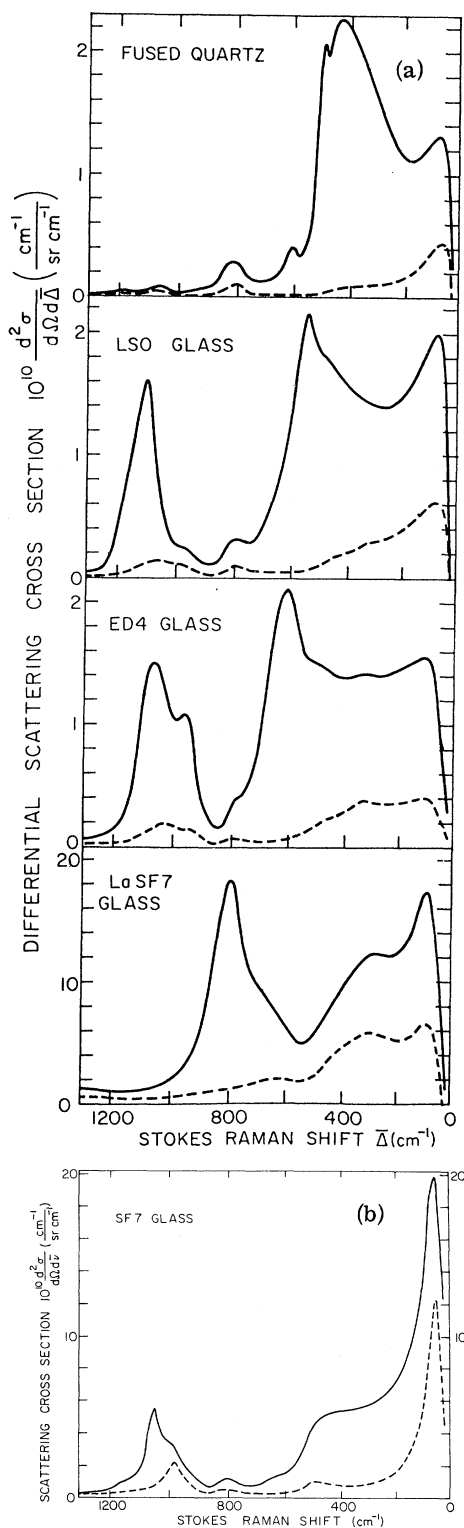


FIG. 1. Differential Raman-scattering cross sections vs (Stokes) frequency shift $\bar{\Delta}$ from 514-nm incident beam for five glasses ($\bar{\Delta} \equiv \Delta / (2\pi c) \text{ cm}^{-1}$). Solid lines are polarized (\parallel) and dashed lines are depolarized (\perp) cross sections. ($d\bar{\nu} \equiv d\bar{\Delta}$.)

TABLE I. Nonlinear polarization parameters defined in text as derived from our Raman data and intensity-induced polarization change (IIPC) measurements. From these are derived the self-focusing index n_2 of Eq. (9) and the fraction f_e of it that is electronic in origin. All quantities are in esu.

Material	n	$10^{16}B_0$ ^a	$10^{16}(A_0+B_0)$ ^a	$10^{15}(\sigma+2B_0)$ ^b	$10^{15}\sigma$	$10^{14}n_2$ [Eq. (4)]	$10^{14}n_2$ (Meas.)	f_e (%)
Fused quartz	1.46	14 ± 2	57 ± 6	31 ± 2	28 ± 2	11 ± 1	18 ± 3 ^c	79 ± 3
LSO glass	1.52	28 ± 3	70 ± 7	46 ± 3	40 ± 3	15 ± 1		81 ± 3
ED-4 glass	1.56	26 ± 3	68 ± 7	57 ± 4	52 ± 4	18 ± 1.3	$\left\{ \begin{array}{l} 26 \pm 3^c \\ 15 \pm 2^d \\ 15 \pm 3^e \end{array} \right.$	85 ± 3
SF-7 glass	1.65	210 ± 20	315 ± 30	202 ± 20	160 ± 20	58 ± 7		79 ± 3
LASF-7 glass	1.93	380 ± 40	540 ± 50	252 ± 25	176 ± 25	61 ± 8		71 ± 3

^a This work.

^b References 1 and 12.

^c Reference 9.

^d Reference 8.

^e Reference 7.

in changing from 514 to 633 nm excitation.⁷ The dispersion in Raman scattering from benzene vapor, observed by Udagawa *et al.*,¹² is also more consistent with the lower dispersion values. With the possibility of a dispersion error in our values of A_Δ and B_Δ noted, we nonetheless feel the balance of evidence supports our neglect of dispersion at our present level of accuracy and our choice of scattering standards.

Our results may be checked against recent measurements of the self-focusing index n_2 for a monochromatic beam. Since the change in refractive index for linear polarization is defined as $n_2\langle E^2(t) \rangle$, we see from (1) and (2) that, in our terms,

$$n_2 = \pi(\frac{3}{2}\sigma + 2A_0 + 2B_0)/n, \quad (9)$$

where n is the linear refractive index. Our predictions for n_2 in Table I (which depend mainly on Owyong's data¹) are seen to be consistent with the absolute, interferometric, time-resolved pulse measurements of Bliss *et al.*,⁹ and also with the interferometric comparisons with liquid CS₂ of Moran *et al.*,¹⁰ both made at 1.06 μm. Ours are, however, about 30% lower than the values obtained

by Levenson⁴ from three-wave mixing experiments near 525 nm. This is possibly due to his less certain calibration. However, as Levenson points out, the electronic nonlinearities (which we note contribute most to n_2) might cause such a dispersion enhancement at such a short wavelength.

Phenomenological theories of n_2 , developed to aid in the design of low- n_2 glasses, have assumed that n_2 is mainly electronic in origin.¹³⁻¹⁵ This is verified by our values in Table I for its electronic fraction f_e , which, according to (9), is $[1 + 4(B_0 + A_0)/(3\sigma)]^{-1}$.

We have used the results of Fig. 1 to calculate both the real and imaginary parts of A_ν and B_ν at all ν , using the prescriptions we have developed here. Copies of these results may be obtained from the authors and will be reproduced in a forthcoming National Bureau of Standards Special Publication "Damage in Laser Materials: 1974" (edited by A. Glass and A. Guenther).

The authors gratefully acknowledge helpful conversations with A. Owyong, A. J. Glass, E. Snitzer, N. Boling, E. Bliss, M. Moran, and R. L. Carman, and thank S. P. S. Porto for the use of his facilities.

*Research supported by the U. S. Atomic Energy Commission under University of California Lawrence Livermore Laboratory subcontract No. 2713005.

¹A. Owyong, IEEE J. Quantum Electron. **9**, 1064 (1973); A. Owyong, Nat. Bur. Stds. Spec. Publ. No. 387 (U. S. GPO, Washington, D. C., 1973); A. Owyong, R. W. Hellwarth, and N. George, Phys. Rev. B **5**, 628 (1972).

²R. W. Hellwarth, Phys. Rev. **130**, 1850 (1963).

³M. D. Levenson, C. Flytzanis, and N. Bloembergen, Phys. Rev. B **6**, 3462 (1972).

⁴M. D. Levenson, IEEE J. Quantum Electron. **QE-10**, 110 (1974).

⁵R. W. Hellwarth, A. Owyong, and N. George, Phys. Rev. A **4**, 4 (1971).

⁶P. D. Maker, R. W. Terhune, and C. M. Savage, Phys.

Rev. Lett. **12**, 507 (1964).

⁷Y. Kato and H. Takuma, J. Opt. Soc. Am. **61**, 347 (1971); J. Chem. Phys. **54**, 5398 (1971).

⁸R. H. Stolen and E. P. Ippen, Appl. Phys. Lett. **22**, 275 (1973).

⁹E. R. Bliss, D. R. Speck, and W. W. Simmons (unpublished).

¹⁰M. Moran, C. She, and R. L. Carman (unpublished).

¹¹H. E. McComb, Phys. Rev. **29**, 525 (1909).

¹²Y. Udagawa, N. Mikami, K. Kaya, and M. Ito, J. Raman Spectrosc. **1**, 341 (1973).

¹³C. C. Wang, Phys. Rev. B **2**, 2045 (1970).

¹⁴J. F. Fournier and E. Snitzer, IEEE J. Quantum Electron. **QE-10**, 473 (1974).

¹⁵N. L. Boling, A. J. Glass, and A. Owyong (unpublished).